

Response to referee comments on acp-2017-1041

O. Dimdore-Miles, P. I. Palmer, and L. P. Bruhwiler

November 5, 2018

We thank the additional referee for their comments and recommendations for making amendments to our manuscript. Below we outline our response to each of the points made in the review and how we have modified the manuscript inline with them.

- **Analytical Formulation of the IPD**

We acknowledge the points raised by the reviewer in relation to our mathematical description of the IPD.

We have provided a full mathematical derivation of the continuous model of the IPD, with only the headline equations left in the main text. Our model is defined as the difference between spatially averaged concentrations over the polar regions. By providing this more extensive derivation we have dispensed with the schematic.

We no longer make the distinction between IPD and IPD_{Δ} as we instead prefer to refer to the continuous metric (which we develop an expression for in the model) and the station based metric (used for the numerical experiments).

The model follows the protocol recommended by the reviewer and builds on the expression given in equation 1 of the manuscript, expressing concentrations at each polar region as a combination of emissions from that region and emissions transported at an earlier time.

This should hopefully clear up the ambiguity with regards to the nature of terms in our previous model. We also follow the recommendation to give the metric as the difference between the time t and a reference time t_0 . We also address the issue regarding inconsistencies in units by providing a conversion factor between emission mass per unit volume and concentration.

- **Technical Comments**

1. p.2 l.54: $53^{\circ} > \text{latitude} > 53^{\circ}$: even though understandable, this writing is clumsy

We have amended the wording of the latitude ranges.

2. section 2.1: observations are not used in the manuscript, apart from their location; this section could be shortened (especially details on instruments, calibration, etc.) and moved to appendix, as well as figure 1

For completeness we wanted to describe how the IPD was defined, and to assure the reader of the inability of the IPD to infer changes in Arctic emission was not due to data accuracy/precision. This section also shows that our model has skill in reproducing the observed IPD.

3. p.5 l.131: a sinus is a mathematical operator with no unit; thus it is not correct to directly add standard deviations (in ppb) to $\sin(\text{latitude})$.

We have reviewed our methodology for the calculation of uncertainties on the IPD and have changed them accordingly, the new method is outlined on lines 127-132 of the revised manuscript.

4. p.5 l.140: "the atmospheric transport fluxes of emissions": this is not clear

This wording has been changed

5. p.6 l.175: "during 1990" should be "during the year 1990"?
this change has been made
6. p.6 l.180: when is the noise? all over the period? is it normal then that the IPDs merge together in 2010 in fig. 6B?
This has been addressed, there was an error in the plotting routine that meant the IPD was plotted for a different number of years in each case. Amended accordingly.
7. p.9 l. 279: please check the date of launch when reaching the proof-reading step as it is regularly postponed.
Checked and amended based on <https://www.wmo-sat.info/oscar/satellites/view/592>.

Detecting changes in Arctic methane emissions: limitations of the inter-polar difference of atmospheric mole fractions

Oscar B. Dimdore-Miles¹, Paul I. Palmer¹, and Lori P. Bruhwiler²

¹School of GeoSciences, University of Edinburgh, Edinburgh, UK

²National Oceanic and Atmospheric Administration, Earth System Research Laboratory, Boulder, Colorado, USA

Correspondence to: P. I. Palmer
(paul.palmer@ed.ac.uk)

Abstract. We consider the utility of the annual inter-polar difference (IPD) as a metric for changes in Arctic emissions of methane (CH₄). The IPD has been previously defined as the difference between weighted annual means of CH₄ mole fraction data collected at ~~polar stations (-53° > latitude > stations from the two polar regions (defined as latitudes poleward of 53°N and 53°S, respectively))~~. This subtraction approach (IPD_Δ) implicitly assumes that extra-polar CH₄ emissions arrive within the same calendar year at both poles. ~~Using an analytic approach we show that a more comprehensive description~~ We show using a continuous version of the IPD ~~includes terms corresponding to the that the metric includes not only changes in Arctic emissions but also terms that represent~~ atmospheric transport of air masses from ~~to~~ lower latitudes to ~~from~~ the polar regions. We show the importance of these atmospheric transport terms in understanding the IPD using idealized numerical experiments with the TM5 global 3-D atmospheric chemistry transport model that is run from 1980 to 2010. A northern mid-latitude pulse in January 1990, which increases prior emission distributions, arrives at the Arctic with a higher mole fraction and $\simeq 12$ months earlier than at the Antarctic. The perturbation at the poles subsequently decays with an e-folding lifetime of $\simeq 4$ years. A similarly timed pulse emitted from the tropics arrives with a higher value at the Antarctic $\simeq 11$ months earlier than at the Arctic. This perturbation decays with an e-folding lifetime of $\simeq 7$ years. These simulations demonstrate that the assumption of symmetric transport of extra-polar emissions to the poles is not realistic, resulting in considerable IPD Δ -variations due to variations in emissions and atmospheric transport. We assess how well the annual IPD can detect a constant annual growth rate of Arctic emissions for three scenarios, 0.5%, 1%, and 2%, superimposed on signals from lower latitudes, including random noise. We find that it can take up to 16 years to detect the smallest prescribed trend in Arctic emissions at the 95% confidence level. Scenarios with higher, but likely unrealistic, growth in Arctic

emissions are detected in less than a decade. We argue that a more reliable measurement-driven approach would require data collected from all latitudes, emphasizing the importance of maintaining a
25 global monitoring network to observe decadal changes in atmospheric greenhouse gases.

1 Introduction

Atmospheric methane (CH_4) is the second most important contributor to anthropogenic radiative forcing after carbon dioxide. Observed large-scale variations of atmospheric CH_4 (Nisbet et al., 2014) have evaded a definitive explanation due to the sparseness of data (Kirschke et al., 2013; Rigby et al., 2016; Turner et al., 2016; Schaefer et al., 2016; Saunio et al., 2016). Atmospheric CH_4 is determined by anthropogenic and natural sources, and by loss from oxidation by the hydroxyl radical (OH) with smaller loss terms from soil microbes and oxidation by Cl. This results in an atmospheric lifetime of $\simeq 10$ years. Anthropogenic CH_4 sources include leakage from the production and transport of oil and gas, coal mining, and biomass burning associated with agricultural
35 practices and land use change. Microbial anthropogenic sources include ruminants, landfills, and rice cultivation. The largest natural source is microbial emissions from wetlands, with smaller but significant contributions from wild ruminants, termites, wildfires, landfills, and geologic emissions (Kirschke et al., 2013; Saunio et al., 2016). Here, we focus on our ability to quantify changes in Arctic emissions using polar atmospheric mole fraction data.

40 Warming trends over the Arctic, approximately twice the global mean (AMAP, 2015), are eventually expected to result in thawing of permafrost. Observational evidence shows that permafrost coverage has begun to shrink (Christensen et al., 2004; Reagan and Moridis, 2007). Arctic soils store an estimated 1700 GtC (Tarnocai et al., 2009). As the soil organic material thaws and decomposes it is expected that some fraction of this carbon will be released to the atmosphere as CH_4 ,
45 depending on soil hydrology. Current understanding is that permafrost carbon will enter the atmosphere slowly over the next century, reaching a cumulative emission of 130–160 PgC (Schoor et al., 2015). If only 2% of this carbon is emitted as CH_4 , annual Arctic emissions could approximately double by the end of the century from current estimates of 25 Tg CH_4/yr inferred from atmospheric inversions (AMAP, 2015). At present, using data from the current observing network there is no
50 strong evidence to suggest large-scale changes in Arctic emissions (Sweeney et al., 2016).

The inter-polar difference (IPD) has been proposed as a sensitive indicator of changes in Arctic emissions that can be derived directly from network observations of atmospheric CH_4 mole fraction. The IPD, as previously defined (Dlugokencky et al., 2003), is the difference between weighted annual means of CH_4 mole fraction data collected at polar stations (~~-53~~those poleward of $\pm 53^\circ$ >
55 latitude $\gg 53^\circ$) such as those from the NOAA Earth System Research Laboratory (ESRL) network (https://www.esrl.noaa.gov/gmd/dv/site/site_table2.php). Data from individual sites are weighted inversely by the ~~sine~~ cosine of the station latitude and by the standard deviation of the data at a par-

ticular site. Hereafter, we denote this subtraction method as IPD_{Δ} to distinguish it from the full description of the IPD, as described below. Dlugokencky et al. (2003) reported an abrupt drop in IPD Δ during the early 1990s. They suggested this magnitude of change was indicative of a 10 Tg CH_4 /yr reduction, which they attribute to the collapse of fossil fuel production in Russia following the 1991 breakup of the Soviet Union (Dlugokencky et al., 2011). In more recent work, Dlugokencky et al. (2011) proposed that the IPD Δ -metric is potentially sensitive to changes in Arctic emissions as small as 3 Tg CH_4 /yr, representing a value of 10% of northern wetland emissions. However, studies have reported little or no increase in IPD Δ between 1995 and 2010 (Figure 1, Dlugokencky et al. (2011, 2003)), a period during which rising Arctic temperatures were expected to lead to an increase in emissions (Mauritsen, 2016; McGuire et al., 2017). In this work, we examine how sensitive the IPD is to changing CH_4 emissions by using model simulations guided by results from an analytical approach.

First, we introduce an analytic model of the atmosphere to demonstrate derive the continuous version of the IPD^C to introduce the atmospheric transport terms involved with the full IPD. We divide the world into three contiguous regions: Arctic, background, and Antarctica (Figure ??); the inter-polar meridional length, defined from the Arctic to the Antarctic, is given by R . We that are not considered in the subtraction approach. For our model, we have a local Arctic source $L(t)$ (mass CH_4 per unit time) and an isolated inter-polar source B (mass CH_4 per unit time) emitted at position r and time t . For simplicity, we assume that there is only one measurement site in the Arctic and one in Antarctica, and have neglected the transport of $L(t)$ to the Antarctic.

The IPD in the general sense is then The IPD^C is given by :

$$IPD_{\Delta}^C(t) = \underbrace{k}_{\text{Signal measured at the Arctic site}} \underbrace{\frac{1}{\Delta r} \int_{r=53}^{90} c(r,t) dr}_{\text{Signal measured at the Antarctic site}} - \underbrace{\frac{1}{\Delta r} \int_{r=-90}^{-53} c(r,t) dr}_{\text{Signal measured at the Antarctic site}}, \quad (1)$$

where τ_N and τ_S denote the time taken for source B Δr is the graduation in latitude in the model and $c(r,t)$ denotes atmospheric CH_4 mole fraction (ppb) at latitude r to reach the Arctic and Antarctic, respectively. The variable k describes the mass to mole fraction conversion, following the mole fraction definition for IPD Δ . The dummy variable r' has been introduced to avoid confusion in the integral. This relationship can be expanded (Appendix A) \div

$$IPD_{\Delta}(t) \equiv \frac{kL(t) + k \left(\int_r^R \frac{dB(t,r')}{dt} \Big|_{t-\tau_S(r')} \tau_S(r') dr' - \int_r^0 \frac{dB(t,r')}{dt} \Big|_{t-\tau_N(r')} \tau_N(r') dr' \right) + k \left(\int_r^0 B(t,r') dr' - \int_r^R B(t,r') dr' \right)}{}$$

The analytical model highlights two grouped terms: the first term represents the integrated response of B as it travels northward and southward to the poles, and time t that includes influences from all other latitudes and previous times. The mole fraction can then be described as:

$$c(r, t) = \int_{t'=-\infty}^{t'=t} \int_{r'=-90}^{90} k(r', t') S(r', t') H_{r', -r}^{t'-t} dr' dt', \quad (2)$$

where $S(r', t')$ denotes the surface emission fluxes ($\text{g cm}^{-2} \text{s}^{-1}$); $H_{r', -r}^{t'-t}$ denotes the fraction of emissions from location r' at initial time t' that contributes to the second term represents differences in the response functions. The IPD_{Δ} definition implicitly assumes these grouped terms are zero. Under these circumstances, there are two limiting cases in which the IPD_{Δ} can isolate $L(t)$ concentration

at location r and a later time t , which includes atmospheric chemistry and transport; and $k(r', t')$ (cm^3/g) describes the conversion between emissions and atmospheric mole fraction (parts per billion, ppb) and takes the form $k(r, t) = \frac{N_a}{M_w \rho(r, t)}$, where N_a and M_w denote Avagadro's constant (molecules/mole) and the molar weight of CH_4 (g/mole), respectively, and $\rho(r, t)$ denote the number density of air (molec cm^{-3}).

Our expression for IPD^C can be reformulated as the difference between values determined at time t and a reference time t_0 . The reader is referred to Appendix A for a full derivation of the expressions used in this introduction. Equation 3 describes the IPD using the assumptions previously used (e.g. Dlugokencky et al. (2003)): 1) emissions from B are constant in time southern polar region contains no local sources, and 2) B arrives at both poles simultaneously with symmetric transport histories. Neither case is realistic on any time scale. Even point sources are often time-dependent. The emissions from the northern polar region are too diffuse after transport between poles to significantly affect mole fractions at the southern polar region.

$$\begin{aligned} \text{IPD}^C(t) - \text{IPD}^C(t_0) &\equiv \frac{1}{\Delta r} \int_{t'=t_0}^{t'=t} \left(\int_{r=53}^{90} \left[\int_{r'=53}^{90} k(r', t') S(r', t') H_{r', -r}^{t'-t} dr' + \right. \right. \\ &\quad \left. \left. \int_{r'=-53}^{53} k(r', t') S(r', t') H_{r', -r}^{t'-t} dr' \right] dr - \right. \\ &\quad \left. \int_{r=-90}^{-53} \int_{r'=-53}^{53} k(r', t') S(r', t') H_{r', -r}^{t'-t} dr' dr \right) dt' \end{aligned} \quad (3)$$

The first integral in equation 3 represents contributions from changes in northern polar sources between t and t_0 ; and the second and third integral represent atmospheric transport terms that describe the contributions from intra polar sources to the northern and southern polar mole fractions, respectively. To successfully isolate local Arctic emissions of CH_4 using the IPD these atmospheric transport terms would have to cancel out. Taking into account that the characteristic timescale for

inter-hemispheric transport of an air mass is $\simeq 1$ year (Holzer and Waugh, 2015). ~~Using the annual IPD Δ (Dlugokencky et al., 2003) we show we argue~~ that only a fortuitous set of circumstances would allow ~~this metric to isolate $L(t)$~~ the IPD as previously defined to isolate local northern polar sources of CH₄.

120 In the next section, we describe the data and methods used previously to define IPD Δ , and the model calculations we use to explore the importance of these atmospheric transport terms, as illustrated in equation ~~??~~3. In section 3, we report the results from our numerical experiments. We conclude in section 4.

2 Data and Methods

125 2.1 Observed and Model IPD Δ

To calculate the IPD Δ , following Dlugokencky et al. (2011), we first group together a subset of NOAA ESRL global monitoring measurement sites that are located $-53^\circ > \text{latitude} > 53^\circ$ (Table 1), and assign them as the North and South polar regions. For each polar region we calculate mean biweekly mole fractions across the stations, weighted inversely by station latitude and the standard
130 deviation about the biweekly mean CH₄ mole fraction. Biweekly values of IPD Δ are then averaged over a calendar year to determine the annual IPD Δ , which has been used in previous studies.

We use biweekly CH₄ values determined from measurements of discrete air samples collected in flasks from the NOAA Cooperative Global Air Sampling Network (NOAA CGASN). Air samples (flasks) are collected at the sites and analysed for CH₄ at NOAA ESRL in Boulder, Colorado using
135 a gas chromatograph with flame 220 ionization detection. Each sample aliquot is referenced to the WMO X2004 CH₄ standard scale (Dlugokencky et al., 2005). Individual measurement uncertainties are calculated based on analytical repeatability and the uncertainty in propagating the WMO CH₄ mole fraction standard scale. Analytical repeatability varies between 0.8 to 2.3 ppb, and has a mean value of approximately 2 ppb averaged over the measurement record. Uncertainty in scale
140 propagation is based on a comparison of discrete flask-air and continuous measurements at the MLO and BRW observatories and has a fixed value 0.7 ppb. These two values are added in quadrature to estimate the total measurement uncertainty, equivalent to a $\simeq 68\%$ confidence interval.

Five northern and two southern polar stations (Table 1) have data that cover the period discussed in previous studies (approximately 1986–2010) and a weekly resolution to calculate biweekly averages.
145 We impute missing data filled using a two-stage approach. We use linear interpolation to replace missing measurements from a given week and year with the average of the measurement values from the same week of the three preceding and subsequent years (to provide a climatological value but preserve long term trends in the data). If corresponding weekly measurements for the six neighbouring years are incomplete, we use a cubic spline interpolation. We calculate the uncertainties on the bi-
150 weekly weighted concentration means from the polar regions using the formula for the standard error

$\sigma_{\bar{x}}$ of a weighted mean μ (Taylor, 1997), $\sigma_{\bar{x}}^2(\mu) = 1 / \sum_i (\frac{1}{\sigma_i + \sin(\phi_i)})^2$ $\sigma_{\bar{x}}^2(\mu) = 1 / \sum_i (\frac{1}{\sigma_i \cos(\phi_i)})^2$, where the denominator represents weights assigned to each station i as a function of biweekly mole fraction standard deviation σ_i and the latitude ϕ_i of the station. We propagate these errors to determine the error on the annual IPD, following Dlugokencky et al. (2011).

155 We calculate the corresponding model IPD Δ -values by sampling TM5 (described below) at the time and location of each NOAA ESRL observation and processing the values as described above for the observations.

2.2 Numerical Experiments

Building on the terms evaluated using our ~~analytical~~ continuous IPD^C model (equation ~~??~~3) we use the TM5 atmospheric transport model (Krol et al., 2005) to 1) examine ~~the atmospheric transport fluxes of emissions~~ how perturbations in inter-polar emissions are transported to the polar regions, and 2) determine the sensitivity of the IPD Δ -to different emission distributions.

For our numerical experiments, we run the TM5 model using a horizontal spatial resolution of 2° (latitude) and 3° (longitude), driven by meteorological fields from the European Center for Medium Range Weather Forecast (ECMWF) ERA-Interim reanalysis. Fossil fuel and agricultural emission estimates are taken from the EDGAR3.2 inventory (Olivier et al., 2005) with modifications (Schwietzke et al., 2016). Natural emissions are based on the prior values used by CarbonTracker-CH₄ (Bergamaschi et al., 2005; Bruhwiler et al., 2014). Bruhwiler et al. (2014) reported posterior CH₄ emission estimates for high northern latitudes that were 20–30% smaller than prior values, which we use in our current experiments. An important consequence of our using these prior values is that the model IPD Δ -values have a positive bias compared to values determined by CH₄ mole fraction measurements.

We run a suite of targeted numerical experiments to test the sensitivity of the IPD Δ -to pulsed and noisy variations from mid-latitude and tropical emission sources. ~~The noise-variation experiments mostly explore the role of the first grouped term in the IPD (equation ??) and the single-pulse experiments mostly explore the role of the second grouped term in the IPD (equation ??).~~ In practice, both sets of experiments integrate information from both ~~grouped atmospheric~~ atmospheric transport terms. We also consider experiments that included Arctic emissions with different constant growth rates and realistic variations in lower latitude emissions. As a control we use a simulation with constant emissions. Appendix B includes a presentation of the time series used to calculate the IPD Δ from our experiments.

We initialize our TM5 numerical experiments from 1980 using initial conditions defined by the observed North-South distribution of CH₄ in the early 1980s. Each experiment is run from 1980 to 2010, with mole fractions sampled at the time and location of the network observations.

185 Control Run

Figure 1 shows that the model IPD Δ for the control run is higher than observed values, as explained above. The model IPD Δ also shows less variability than observed values. Variations of IPD Δ in the early 1990s have been attributed to a rapid decline in fossil fuel production following the 1991 breakup of the Soviet Union (Dlugokencky et al., 2011). We determine the model response
190 to changes in emissions (as described below) by subtracting the control run from the perturbed emissions runs.

Pulsed Emission Runs

To investigate the impact of a sustained continental-scale change in emissions on the weighted polar means and the IPD Δ metric, we run the control experiment configuration but during the year 1990
195 we increase emissions by an amount that is evenly distributed throughout the year. In the first pulse experiment, we increase existing mid-latitude emissions over the contiguous USA by 10 Tg CH₄. In the second experiment, we increase existing tropical land sources (within $\pm 30^\circ$) by 20 Tg CH₄. We present polar mole fraction time series produced using the control and pulsed experiments shown in Appendix B.

200 Random Noise Emission Runs

To investigate the role of intra- and inter- annual variations of emission sources on the IPD Δ we re-run the two pulse experiments but superimpose standard uniform distribution noise $\mathcal{U}(0,1)$ on the emissions. We conduct two runs of TM5: one with a noise function of amplitude 10 Tg on US emissions and another with a function of amplitude 20 Tg on tropical sources. These experiments
205 help us to determine the observability of changes in mid-latitude and tropical sources at the poles and whether the IPD Δ ~~can isolate $L(t)$~~ can isolate local Arctic emission.

Arctic Emission Variation

To investigate the ability of IPD Δ to detect a constant annual growth rate of Arctic emissions, we use the control experiment configuration but in three separate experiments we increase Arctic
210 emission by 0.5%, 1% and 2% on an annual basis. Emissions are mostly limited to summer months (June–August) when the soil surface is typically not frozen.

3 Results

Figure 2 summarizes the results from our pulsed emission experiments. The model response at both poles to the 1990 pulse peaks rapidly and then falls off approximately exponentially over several
215 years. The Northern Region tracer represents the sum of $L(t)$ ~~and the second and third atmospheric~~

~~transport terms in equation ??~~ local Arctic emissions and the first atmospheric transport term in equation 3, and the Southern Region tracer represents the ~~first and fourth atmospheric transport terms~~ second atmospheric transport term in that equation.

Figure 2A shows that the mid-latitude pulse of 10 Tg CH₄ results in a larger change at the northern polar stations (7.3 ppb peak) than at the southern polar stations (3.0 ppb peak). This reflects the longer transport time for the pulse to reach the southern stations during which time the pulse becomes more diffuse. More importantly, for the interpretation of the IPD Δ we find that the northern polar stations experience the majority of the pulse 0.96 years before the southern polar stations. After 1991 the pulse responses decay with e-folding lifetimes of 4.43 years and 8.94 years in the Northern and Southern polar stations, respectively. Figure 2C shows that the difference in pulse response at the poles decays from a maximum value in 1992 with an e-folding time of approximately 0.36 years.

Figure 2B shows that the peak of the 20 Tg CH₄ tropical pulse reaches the southern polar region 0.92 years earlier than the northern polar region. This results in a larger change in southern polar CH₄ mole fractions (8.3 ppb peak) compared to corresponding values over the northern polar regions. The earlier transit of the tropical pulse to the southern polar region reflects that much of the prior tropical CH₄ fluxes that we perturb lie in the southern hemisphere. Responses to the tropical pulse decay after 1992 with e-folding lifetimes of 8.65 years and 7.07 years for the northern and southern regions, respectively. The significant transport delay and disparity in responses means that an annual mean subtraction of northern and southern polar stations (IPD Δ) will not remove the influence of the mid-latitude pulse and isolate $E(t)$ local Arctic CH₄ emissions as previously assumed.

Figure 3A shows that signal variations that we might expect from the atmospheric transport of intra- and inter- annual variations changes in emission sources (~~first grouped term in equation ??~~) can dominate the IPD Δ signal. In response to noise superimposed on mid-latitude USA emissions, changes in biweekly IPD Δ values have a mean value of 3.0 ppb (range -0.1–6.0 ppb). The corresponding changes in the annual IPD Δ has a mean value of 3.0 ppb (range 0.3–5.4 ppb). The response of the biweekly IPD Δ to noise on tropical emissions have a mean value of -2.8 ppb (range -12.8–5.6 ppb) and the corresponding response to the annual IPD Δ has a mean value of -2.7 ppb (range -4.7–0.6 ppb). These experiments show that the IPD Δ is susceptible to variations in inter-polar sources.

Figure 3B shows that IPD Δ is sensitive to changes in $E(t)$ local Arctic CH₄ emissions, as expected, with a near-perfect correlation. We find only a modest response of IPD Δ to large percentage increases in Arctic emissions: annual increases of 0.5%, 1%, and 2% in Arctic emissions result in changes of 0.09, 0.17 and 0.35 ppb per year in IPD Δ . IPD Δ . IPD variations that might be expected from intra- and inter- annual variations in mid-latitude and tropical sources are typically much larger than the signal associated with changes in $E(t)$ local Arctic emissions. We find that the IPD Δ in the presence of a constant Arctic annual growth rate and intra- and inter- variations in mid-latitude and tropical emissions can detect a 0.5% annual growth rate within 11–16 years to 95% confidence level

(Weatherhead et al., 1998). Table 2 summarizes our results for different growth rates but generally the larger the Arctic growth rate the shorter it takes to detect the signal, as expected. The IPD Δ is more susceptible to variations in northern mid-latitude sources than tropical sources, as described above. These results represent a best-case scenario for the IPD Δ . In practice, there are also intra- and inter- annual variations associated with $L(t)$ -local Arctic emissions that will complicate the interpretation of the IPD Δ and likely increase the time necessary to detect a statistical significant signal.

260 4 Concluding Remarks

We critically assessed the inter-polar difference (IPD) as a robust metric for changes in Arctic emissions. The IPD has been previously defined as the difference between weighted means of atmospheric CH₄ time series collected in the northern and southern polar regions (IPD Δ). A comprehensive definition. A continuous version of the IPD ^C model includes at least two additional terms associated with atmospheric transport. Using the TM5 atmospheric transport model we highlighted the importance of these atmospheric transport terms. We showed that IPD Δ has a limited capacity to isolate changes in Arctic emissions.

We show that an inter-polar emission (here, we have evaluated emissions from midlatitudes and the tropics) generally arrives at one pole earlier the other pole by approximately one year, invalidating a key assumption of the IPD Δ . We also show that a small amount of noise on prior mid-latitude or tropical sources that might be expected due to intra- and inter- annual source variations is not removed in the calculation of the IPD Δ . While the IPD Δ can detect a constant Arctic annual growth rate of emissions, any additional variation due to mid-latitude or tropical sources can delay detection of a statistical significant signal by up to 16 years.

Our study highlights the need for sustaining a spatially distributed and intercalibrated observation network for the early detection of changes in Arctic CH₄ emissions. The ability to detect and quantify trends in these emissions directly from observations is attractive, but in reality we need to account for variations in extra-polar fluxes and differential atmospheric transport rates to the poles. This effectively demands the use of a model of atmospheric transport, which must be assessed using global distributed observations.

A Bayesian inference method that integrates information from prior knowledge and measurements is an ideal approach for quantifying changes in Arctic CH₄ emissions, but assumes a) reliable characterization of model error and b) measurements that are sensitive to all major sources. Model error characterization is an ongoing process. Estimating CH₄ emissions from atmospheric measurements is an undetermined (i.e., number of fluxes to be estimated \gg number of observations available) and an ill-posed (i.e., several different solutions exist that are equally consistent with the available measurements) inverse problem. Prior emissions are required to regularize the inverse problem, allowing

posterior fluxes to be determined that are consistent with prior knowledge and atmospheric CH₄ measurements, and their respective uncertainties. Ground-based measurements represent invaluable
290 information to determine atmospheric variations of CH₄, but the spatial density of these data limits the resolution of corresponding posterior emission estimates to long temporal and large spatial scales. Column observations from satellites represent new, finer-scale information about atmospheric CH₄, but they are generally less sensitive to surface processes than ground-based data. Daily global observations of atmospheric CH₄ from the latest of these satellite instruments, TROPOMI aboard
295 Sentinel-5P (launched in late 2017), promise to confront current understanding about Arctic emissions of CH₄ described by land-surface models and bottom-up emission inventories. Passive satellite sensors, such as TROPOMI, rely on reflected sunlight so they are limited by cloudy scenes and by low-light conditions during boreal winter months. Active space-borne sensors (e.g. Methane Remote Sensing Lidar Mission, MERLIN, due for launch in > 2021) that employ onboard lasers to
300 make measurements of atmospheric CH₄ have the potential to provide useful observations day and night and throughout the year over the Arctic. The sensitivity of MERLIN to projected changes in Arctic emissions of CH₄ is still to be determined. Another major challenge associated with satellite observations is cross-calibrating sensors to develop self-consistent timeseries that can be used to
305 <5 years). Even with access to all these data, it is clear that no simple, robust data metric exists without integrating the effects of atmospheric transport, but data-led analyses remains critical for underpinning knowledge of current and future changes in Arctic CH₄ emissions.

Acknowledgements. O.B.D. was funded by summer undergraduate project via the NERC Greenhouse gAs Uk and Global Emissions (GAUGE) project (grant NE/K002449/1). P.I.P. gratefully acknowledges his Royal Society Wolfson Research Merit Award. We thank NOAA/ESRL for the CH₄ surface mole fraction data which is
310 provided by NOAA/ESRL PSD, Boulder, Colorado, USA, from their website <http://www.esrl.noaa.gov/psd/>.

References

- AMAP: AMAP Assessment 2015: Methane as an Arctic climate forcer, Tech. rep., Arctic Monitoring and Assessment Programme (AMAP), Oslo, Norway, 2015.
- 315 Bergamaschi, P., Krol, M., Dentener, F., Vermeulen, A., Meinhardt, F., Graul, R., Ramonet, M., Peters, W., and Dlugokencky, E.: Inverse modelling of national and European CH₄ emissions using the atmospheric zoom model TM5, *Atmosphere Chemistry and Physics*, 5, 2431–2460, 2005.
- Bruhwyler, L., Dlugokencky, E., Masarie, K., Ishizawa, M., Andrews, A., Miller, J., Sweeney, C., Tans, P., and Worthy, D.: CarbonTracker-CH₄: an assimilation system for estimating emissions of atmospheric methane, 320 *Atmosphere Chemistry and Physics*, 14, 8269–8293, 2014.
- Christensen, T., Johansson, T., Ákerman, H., Mastepanov, M., Malmer, N., Friborg, T., Crill, P., and Svensson, B.: The role of methane in global warming: where might mitigation strategies be focused?, *Geophysical Research Letters*, 31, 2004.
- Dlugokencky, E., S.Houweling, Bruhwiler, L., Masarie, K., Lang, P., Miller, J., and Tansy, P. P.: Global atmospheric methane: budget, changes and dangers, *Geophysical Research Letters*, 30, 2003.
- 325 Dlugokencky, E., Nisbet, E., Fisher, R., and Lowry, D.: Global atmospheric methane: budget, changes and dangers, *Philosophical Transactions of the Royal Society*, 369, 2058–2072, 2011.
- Dlugokencky, E. J., Myers, R. C., Lang, P. M., Masarie, K. A., Crotwell, A. M., Thoning, K. W., Hall, B. D., Elkins, J. W., and Steele, L. P.: Conversion of NOAA atmospheric dry air CH₄ mole fractions to 330 a gravimetrically prepared standard scale, *Journal of Geophysical Research: Atmospheres*, 110, n/a–n/a, doi:10.1029/2005JD006035, <http://dx.doi.org/10.1029/2005JD006035>, d18306, 2005.
- Holzer, M. and Waugh, D. W.: Interhemispheric transit time distributions and path-dependent lifetimes constrained by measurements of SF₆, CFCs, and CFC replacements, *Geophysical Research Letters*, 42, 4581–4589, doi:10.1002/2015GL064172, <http://dx.doi.org/10.1002/2015GL064172>, 2015GL064172, 2015.
- 335 Kirschke, S., Bousquet, P., Ciais, P., and Saunois, M.: Three decades of global methane sources and sinks, *Nature Geoscience*, 6, 813–823, 2013.
- Krol, M., Houweling, S., Bregman, B., van den Broek, M., Segers, A., van Velthoven, P., Peters, W., Dentener, F., and Bergamaschi, P.: The two-way nested global chemistry-transport zoom model TM5: algorithm and applications, *Atmospheric Chemistry and Physics*, 5, 417–432, doi:10.5194/acp-5-417-2005, <https://www.atmos-chem-phys.net/5/417/2005/>, 2005.
- 340 Mauritsen, T.: Greenhouse warming unleashed, *Nature Geoscience*, 9, 271–272, 2016.
- McGuire, A., Kelly, B., Guy, L. S., Wiggins, H., Bruhwiler, L., Frederick, J., Huntington, H., Jackson, R., Macdonald, R., Miller, C., Olefeldt, D., Schuur, E., , and Turetsky, M.: Final Report: International Workshop to Reconcile Methane Budgets in the Northern Permafrost Region., Arctic Research Consortium of the United States (ARCUS), Fairbanks, Alaska., p. 14 pages, 2017.
- 345 Nisbet, E., Dlugokencky, E., and Bousquet, P.: Methane on the Rise, Again, *Science*, 343, 493–494, 2014.
- Olivier, J., Aardenne, J. V., Dentener, F., Pagliari, V., Ganzeveld, L., and Peters, J.: Recent trends in global greenhouse gas emissions: regional trends 1970–2000 and spatial distribution of key sources in 2000, *Environmental Science*, 2, 81–99, 2005.
- 350 Reagan, M. and Moridis, G.: Oceanic gas hydrate instability and dissociation under climate change scenarios, *Geophysical Research Letters*, 34, 2283–2292, 2007.

- Rigby, M., Montzka, S., Prinn, R., White, J., Young, D., O'Doherty, S., Lunt, M., Ganesane, A., Manning, A., Simmonds, P., Salameh, P., Hart, C., Mühleg, J., Weiss, R., Fraser, P., Steele, L., Krummel, P., McCulloch, A., and Park, S.: Role of atmospheric oxidation in recent methane growth, *Proceedings of the National Academy of Sciences of the United States of America*, 114, 5373-5377, 2016.
- 355 Saunois, M., Bousquet, P., Poulter, B., Peregon, A., and et al., P. C.: The global methane budget 2000–2012, *Earth System Science Data*; Katlenburg-Lindau, 8, 697–751, 2016.
- Schaefer, H., Fletcher, S. E. M., Veidt, C., Lassey, K. R., Brailsford, G. W., Bromley, T. M., Dlugokencky, E. J., Michel, S. E., Miller, J. B., Levin, I., Lowe, D. C., Martin, R. J., Vaughn, B. H., and White, J. W. C.: A 21st century shift from fossil-fuel to biogenic methane emissions indicated by $^{13}\text{CH}_4$, *Science*, doi:10.1126/science.aad2705, 2016.
- 360 Schuur, E. A. G., McGuire, A. D., Schadel, C., Grosse, G., Harden, J. W., Hayes, D. J., Hugelius, G., Koven, C. D., Kuhry, P., Lawrence, D. M., Natali, S. M., Olefeldt, D., Romanovsky, V. E., Schaefer, K., Turetsky, M. R., Treat, C. C., and Vonk, J. E.: Climate change and the permafrost carbon feedback, *Nature*, 520, 171–179, doi:10.1038/nature14338, 2015.
- 365 Schwietzke, S., Sherwood, O. A., Bruhwiler, L. M. P., Miller, J. B., Etiope, G., Dlugokencky, E. J., Michel, S. E., Arling, V. A., Vaughn, B. H., White, J. W. C., and Tans, P. P.: Upward revision of global fossil fuel methane emissions based on isotope database, *Nature*, 538, 88–91, doi:doi:10.1038/nature19797, 2016.
- Sweeney, C., Dlugokencky, E., Miller, C. E., Wofsy, S., Karion, A., Dinardo, S., Chang, R. Y.-W., Miller, J. B., Bruhwiler, L., Crotwell, A. M., Newberger, T., McKain, K., Stone, R. S., Wolter, S. E., Lang, P. E., and Tans, P.: No significant increase in long-term CH_4 emissions on North Slope of Alaska despite significant increase in air temperature, *Geophysical Research Letters*, 43, 6604–6611, doi:10.1002/2016GL069292, <http://dx.doi.org/10.1002/2016GL069292>, 2016GL069292, 2016.
- 370 Tarnocai, C., Canadell, J. G., Schuur, E. A. G., Kuhry, P., Mazhitova, G., and Zimov, S.: Soil organic carbon pools in the northern circumpolar permafrost region, *Global Biogeochemical Cycles*, 23, n/a–n/a, doi:10.1029/2008GB003327, <http://dx.doi.org/10.1029/2008GB003327>, gB2023, 2009.
- Taylor, J.: *Introduction To Error Analysis: The Study of Uncertainties in Physical Measurements*, University Science Books, 2nd edn., 1997.
- Turner, A., Frankenberg, C., Wennberg, P., and Jacob, D.: Ambiguity in the causes for decadal trends in atmospheric methane and hydroxyl, *Proceedings of the National Academy of Sciences of the United States of America*, 114, 5367-5372, 2016.
- 380 Weatherhead, E. C., Reinsel, G. C., Tiao, G. C., Meng, X.-L., Choi, D., Cheang, W.-K., Keller, T., DeLuisi, J., Wuebbles, D. J., Kerr, J. B., Miller, A. J., Oltmans, S. J., and Frederick, J. E.: Factors affecting the detection of trends: Statistical considerations and applications to environmental data, *Journal of Geophysical Research: Atmospheres*, 103, 17 149–17 161, 1998.
- 385

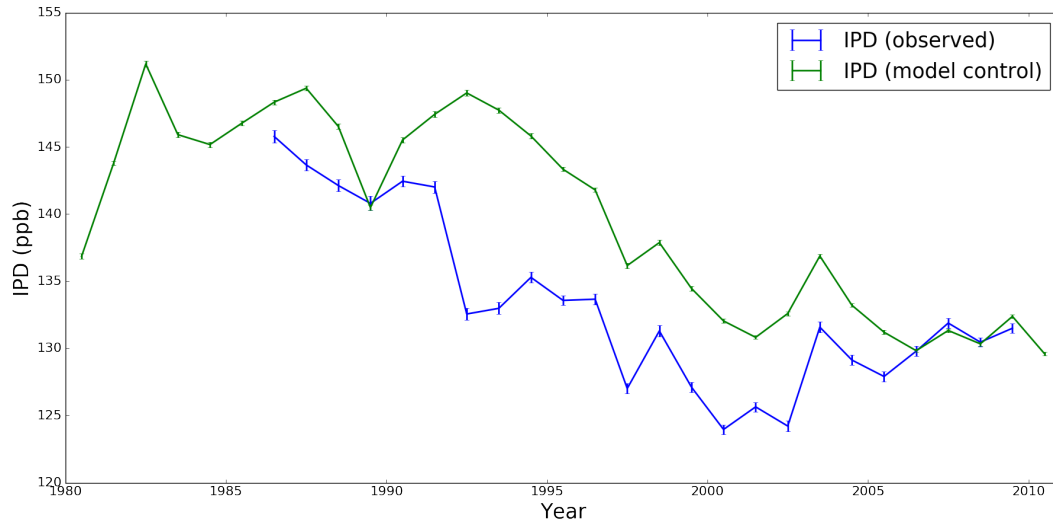


Figure 1. Annual mean IPD Δ -values (ppb) determined by NOAA ESRL and TM5 model atmospheric CH₄ mole fractions using data collected at seven geographical locations (Table 1). Vertical bars denote the one standard deviation associated with the annual mean.

Schematic to describe how an inter-polar source $B(t,r)$ would be viewed at measurement sites in the Arctic and Antarctic:

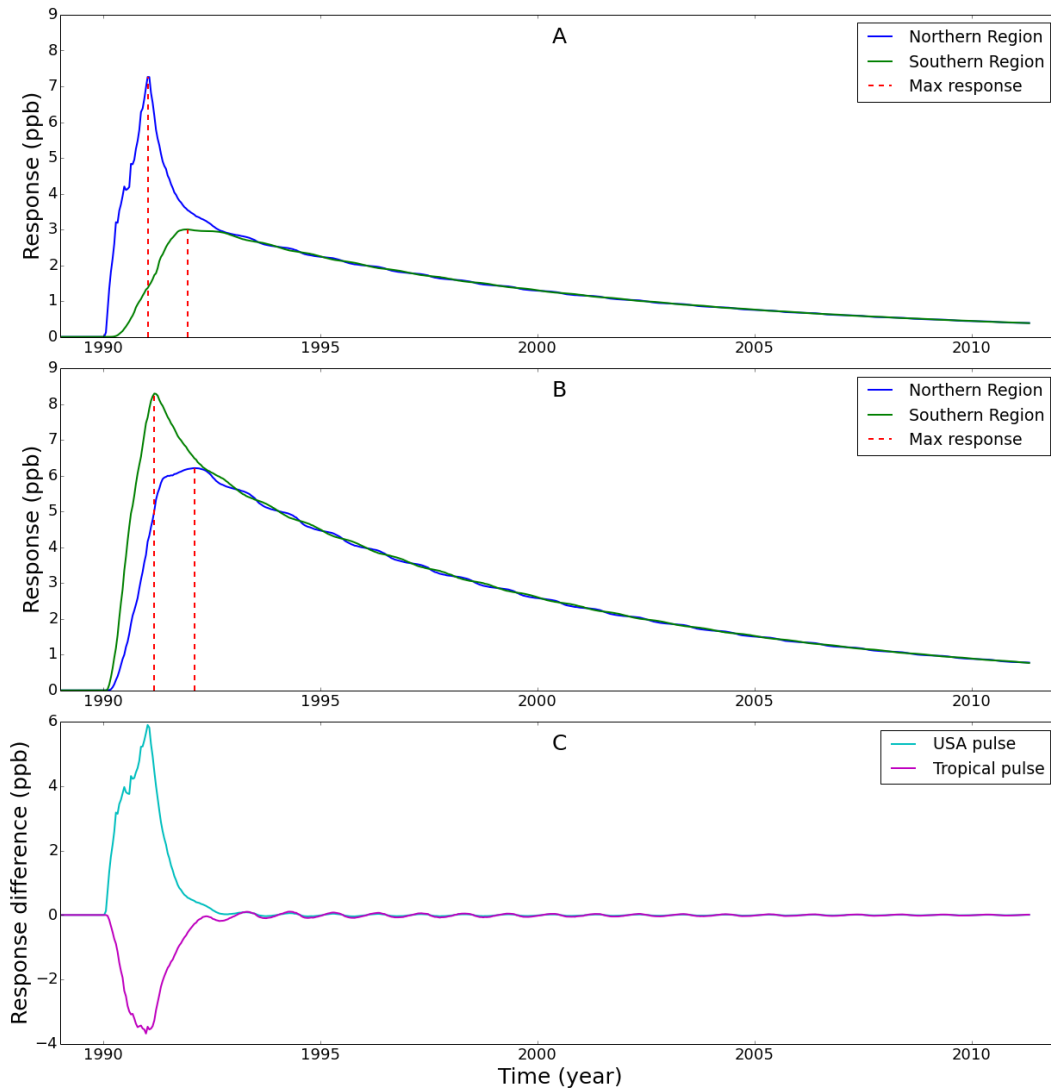


Figure 2. The model response of atmospheric CH₄ mole fraction sampled at northern and southern polar regions to a pulsed emission at (A) mid-latitude USA and (B) the tropics. Panel C shows the IPD response to these mid-latitude and tropical perturbations. In the interest of clarity, we omit error bars from the plots. Vertical red dashed lines denote the peak response time for each polar region.

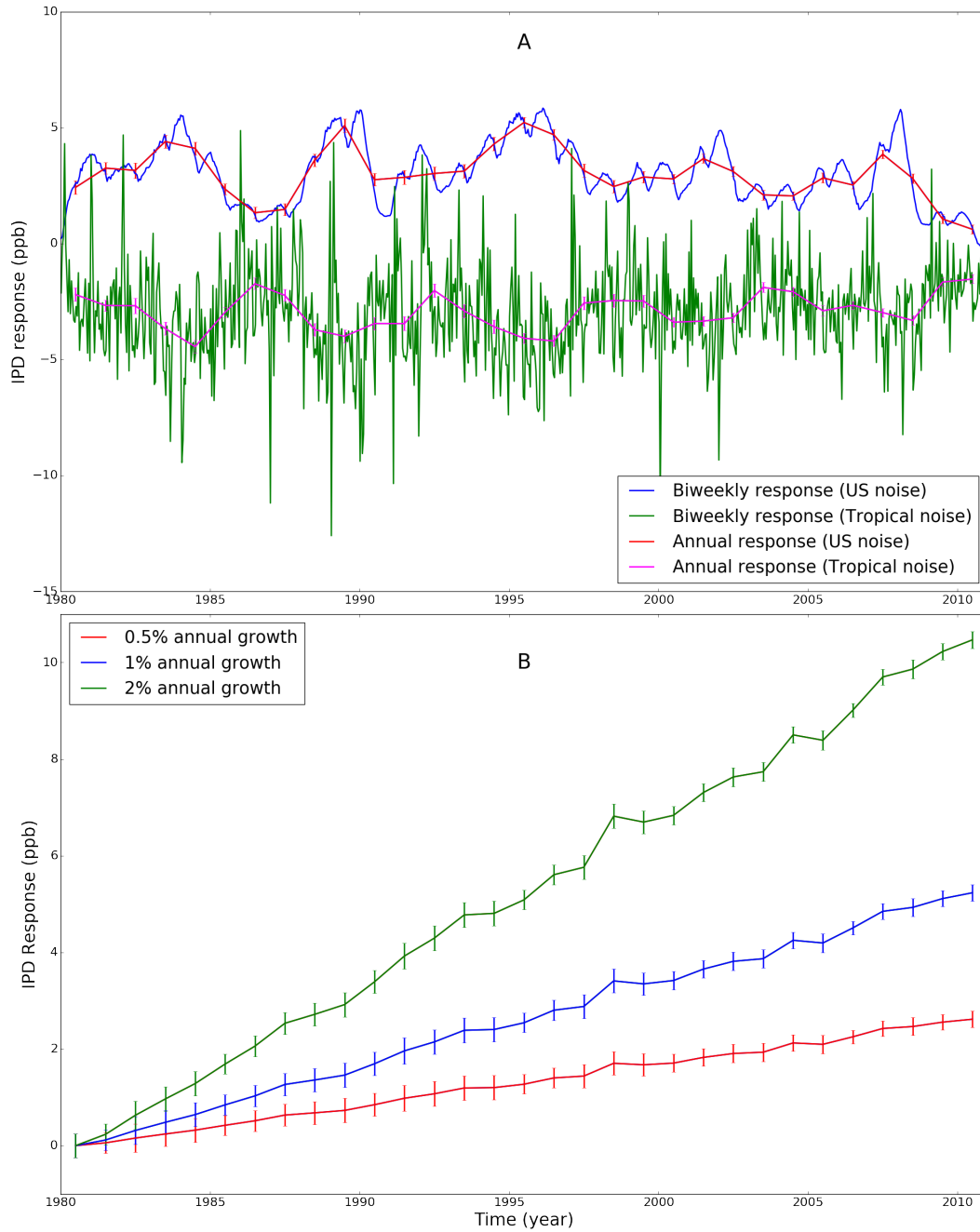


Figure 3. (A) Biweekly and annual model response of the IPD Δ to changes in standard uniform distribution of random noise on prior mid-latitude USA and tropical emissions. (B) annual mean response of IPD Δ to constant growth of Arctic emissions. Vertical lines denote uncertainties on responses.

Table 1. Details of the polar station used to calculate the IPD Δ .

Station Name	Abbreviation	Latitude (°)	Longitude (°)	Altitude (m)
Barrow, Alaska	BRW	71.32	-156.61	11.0
Alert, Canada	ALT	82.45	-62.51	190.0
Cold Bay, Alaska	CBA	55.21	-162.72	21.3
Ocean Station M, Norway	STM	66.00	2.00	0.0
Shemya Island, Alaska	SHM	52.71	174.13	23.0
South Pole, Antarctica	SPO	-89.98	-24.80	2810.0
Palmer Station, Antarctica	PSA	-64.92	-64.00	10.0

Table 2. Number of years required to detect a statistically significant trend in Arctic emissions in the presence of inter-polar emission variations.

Arctic Emission Annual Growth rate	Inter-polar Variation	Years to detect trend in IPD Δ
0.5%	USA (10 Tg amplitude random noise)	16.3
	Tropics (20 Tg amplitude random noise)	10.9
1.0%	USA (10 Tg amplitude random noise)	10.3
	Tropics (20 Tg amplitude random noise)	6.9
2.0%	USA (10 Tg amplitude random noise)	6.5
	Tropics (20 Tg amplitude random noise)	4.3

Appendix A: Development of **Analytical Model for the continuous IPD model**

Here, we include the additional steps required to derive equation ?? in the main text. At a time t the generalized

390 IPD is given by:-

$$\underline{IPD(t) = L(t) + \int_r^0 B(t - \tau_N(r'), r') dr' - \int_r^R B(t - \tau_S(r'), r') dr'}$$

In practice, the response function B that describes the northward and southward transport pathways will be different. First, the fraction of emitted mass going northward will be different to the fraction going southward. Second, in the absence of any additional sources that lie between r and each pole the atmospheric transport mechanisms

395 acting on the southward and northward air mass will be different. We have chosen to neglect these effects, although to some extent differences in atmospheric transport differences are crudely described by τ_N and τ_S .

Combining $IPD(t)$ and $c(t)$ described in equations 1 and 2 results in two integral terms that underpin the continuous version of the IPD:

$$\begin{aligned} \underline{IPD^C(t)} \cong & \frac{1}{\Delta r} \int_{t'=-\infty}^{t'=t} \left(\int_{r=53}^{90} \int_{r'=-90}^{90} k(r', t') S(r', t') H_{r', -r}^{t'-t} dr' dr \right. \\ & \left. - \int_{r=-90}^{-53} \int_{r'=-90}^{90} k(r', t') S(r', t') H_{r', -r}^{t'-t} dr' dr \right) dt' \end{aligned} \quad (A1)$$

The first integral describes contributions to CH_4 mole fractions in the Arctic region, including local emissions and atmospheric transport that originate outside the Arctic emitted at an earlier time t' . The second integral describes contributions to Antarctic CH_4 mole fractions. Both terms are integrated over all previous times so they include the influence from older sources.

405 We can perform a time expansion of the two integral terms as follows:-

$$\underline{B((t + dt), r') = B(t, r') + \left. \frac{dB(t, r')}{dt} \right|_{t+dt, r'} dt.}$$

We now split the first integral into contributions from local Arctic emissions and those transported from sources outside the Arctic, and split the Antarctic term in a similar way:

$$\begin{aligned} \underline{IPD^C(t)} \cong & \frac{1}{\Delta r} \int_{t'=-\infty}^{t'=t} \left(\int_{r=53}^{90} \left[\int_{r'=53}^{90} k(r', t') S(r', t') H_{r', -r}^{t'-t} dr' + \int_{r'=-90}^{53} k(r', t') S(r', t') H_{r', -r}^{t'-t} dr' \right] dr - \right. \\ & \left. \int_{r=-90}^{-53} \left[\int_{r'=-90}^{-53} k(r', t') S(r', t') H_{r', -r}^{t'-t} dr' + \int_{r'=-53}^{90} k(r', t') S(r', t') H_{r', -r}^{t'-t} dr' \right] dr \right) dt' \end{aligned} \quad (A2)$$

Assuming a slow-varying source $B(t)$ (comparable or slower than transport timescales) we can use that expansion:-

$$\underline{IPD(t)} \equiv \frac{L(t) + \int_r^0 \left(B(t, r') - \frac{dB(t, r')}{dt} \Big|_{t-\tau_N(r')} \tau_N(r') \right) dr'}{\frac{- \int_r^R \left(B(t, r') - \frac{dB(t, r')}{dt} \Big|_{t-\tau_S(r')} \tau_S(r') \right) dr'}$$

415 We can then describe the IPD as:-

$$\underline{IPD(t)} \equiv \frac{L(t) + \left(\int_r^R \frac{dB(t, r')}{dt} \Big|_{t-\tau_S(r')} \tau_S(r') dr' - \int_r^0 \frac{dB(t, r')}{dt} \Big|_{t-\tau_N(r')} \tau_N(r') dr' \right) + \left(\int_r^0 B(t, r') dr' - \int_r^R B(t, r') dr' \right)}{\dots}$$

420 The first grouped term describes the integrated response of the source term B as it is transported from the point of emission r . We assume the only source outside of the Arctic is at -53° . We assume that the Antarctic region (south of latitude -53°) contains no local sources so that mole fractions are determined exclusively by atmospheric transport. This eliminates the third term and reduces the integral limits in the second integral. We also assume that atmospheric transport of Arctic sources are too diffuse by the time they arrive at the Antarctic to contribute significantly to Antarctic mole fractions, i.e. $H_{r'-r}^{t'-t} = 0$ for $53^\circ < r' < 90^\circ$ and $-90^\circ < r$ so the second grouped term becomes zero. Note that with differences in the response functions, as described above, the second grouped term would be non-zero and further invalidate the use of $IPD_{\Delta < -53^\circ}$. Using these assumptions A2 now becomes:

$$\underline{IPD^C(t)} \approx \frac{1}{\Delta r} \int_{t'=-\infty}^{t'=t} \left(\int_{r=53}^{90} \left[\int_{r'=53}^{90} k(r', t') S(r', t') H_{r'-r}^{t'-t} dr' + \int_{r'=-53}^{53} k(r', t') S(r', t') H_{r'-r}^{t'-t} dr' \right] dr - \int_{r=-90}^{-53} \int_{r'=-53}^{53} k(r', t') S(r', t') H_{r'-r}^{t'-t} dr' dr \right) dt' \quad (A3)$$

430 Equation A3 includes three terms: 1) influence of local Arctic emissions on Arctic mole fractions; 2) an atmospheric transport term describing the influence of intra-polar sources (between latitudes -53° and $+53^\circ$) on Arctic mole fractions; and 3) an atmospheric transport term describing the influence of intra-polar sources (between latitudes -53° and $+53^\circ$) on Antarctic mole fractions.

If we now consider the change in IPD between some time t and a reference time t_0 we can eliminate the need to integrate over all previous times, and instead evaluate the integrals between t_0 and t .

$$\begin{aligned}
 435 \quad IPD^C(t) - IPD^C(t_0) &= \frac{1}{\Delta r} \int_{t'=-\infty}^{t'=t} \left(\int_{r=53}^{90} \left[\int_{r'=53}^{90} k(r',t')S(r',t')H_{r',-r}^{t'-t} dr' + \right. \right. \\
 &\quad \left. \left. \int_{r'=-53}^{53} k(r',t')S(r',t')H_{r',-r}^{t'-t} dr' \right] dr - \int_{r=-90}^{-53} \int_{r'=-53}^{53} k(r',t')S(r',t')H_{r',-r}^{t'-t} dr' dr \right) dt' - \\
 &\quad \frac{1}{\Delta r} \int_{t'=-\infty}^{t'=t_0} \left(\int_{r=53}^{90} \left[\int_{r'=53}^{90} k(r',t')S(r',t')H_{r',-r}^{t'-t_0} dr' + \int_{r'=-53}^{53} k(r',t')S(r',t')H_{r',-r}^{t'-t_0} dr' \right] dr - \right. \\
 &\quad \left. \int_{r=-90}^{-53} \int_{r'=-53}^{53} k(r',t')S(r',t')H_{r',-r}^{t'-t_0} dr' dr \right) dt' \tag{A4}
 \end{aligned}$$

This can then be expressed as

$$\begin{aligned}
 440 \quad IPD^C(t) - IPD^C(t_0) &= \frac{1}{\Delta r} \int_{t'=t_0}^{t'=t} \left(\int_{r=53}^{90} \left[\int_{r'=53}^{90} k(r',t')S(r',t')H_{r',-r}^{t'-t} dr' + \right. \right. \\
 &\quad \left. \left. \int_{r'=-53}^{53} k(r',t')S(r',t')H_{r',-r}^{t'-t} dr' \right] dr - \int_{r=-90}^{-53} \int_{r'=-53}^{53} k(r',t')S(r',t')H_{r',-r}^{t'-t} dr' dr \right) dt' \tag{A5}
 \end{aligned}$$

In this final expression, the terms that describe local Arctic emissions and atmospheric transport are integrated between the current time t and some reference time. As a result, the emission term gives a measure of changes in Arctic emissions between t and t_0 .

445 Appendix B: IPD plots

For completeness, here we include the plots that complement the analysis reported in the main text. Figure 4 shows the model CH₄ mole fraction corresponding to the weighted mean values at northern and southern polar region used to calculate the IPD Δ in the control and pulsed experiments using the TM5. Figure 5 shows values of the annual mean IPD Δ corresponding to our numerical experiments.

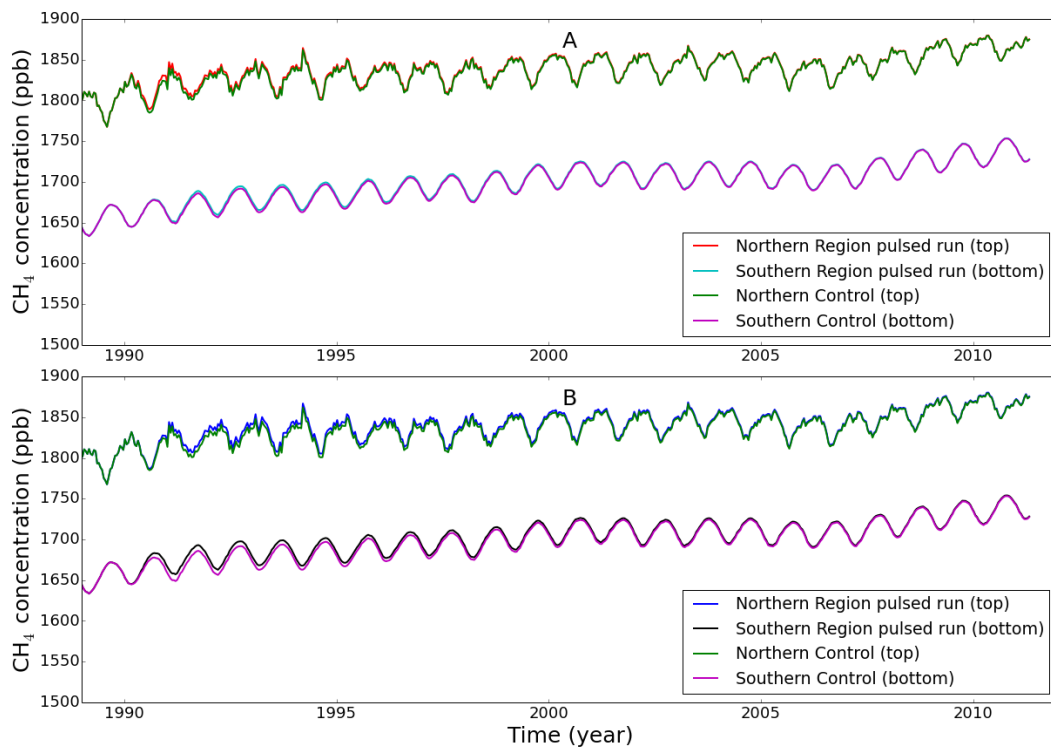


Figure 4. TM5 model CH₄ mole fractions (ppb) sampled at polar regions (Table 1) and weighted inversely by station latitude and standard deviation of the data at that site (see main text). Panel A shows the response of a 10 Tg pulse over mid-latitude USA in 1990 over the northern and southern pole. Panel B shows the response of a 20 Tg pulse over the tropics during 1990.

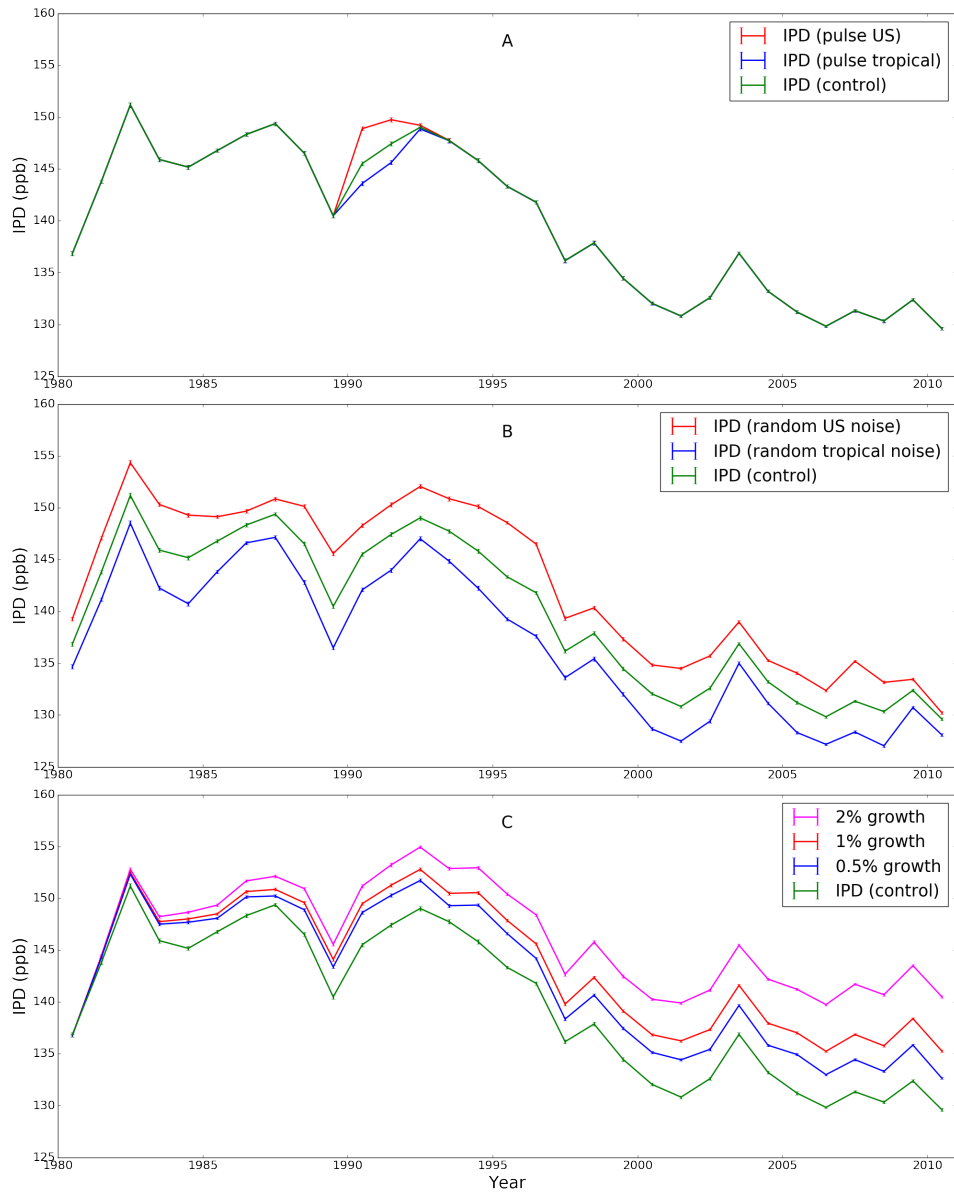


Figure 5. The model IPD \triangle corresponding to the control and all the sensitivity experiments described in the main text.